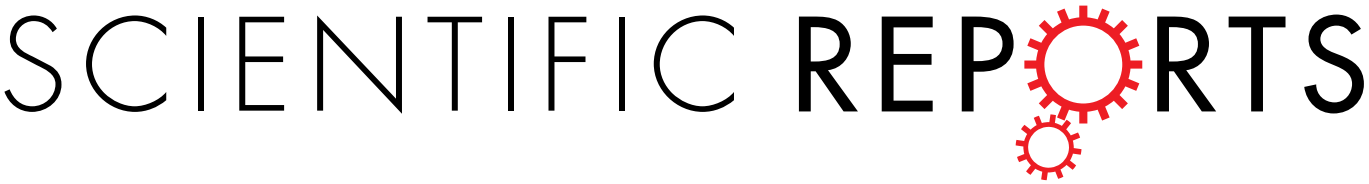

OPEN

A Highly Similar Mathematical Model for Cerebral Blood Flow Velocity in Geriatric Patients with Suspected Cerebrovascular Disease

Received: 01 June 2015
Accepted: 01 October 2015
Published: 26 October 2015

Bo Liu[1,2,4,5,*], Qi Li[3,4,5,*], Jisheng Wang[1], Hu Xiang[1], Hong Ge[1], Hui Wang[1] & Peng Xie[1,2,3,4,5]

Cerebral blood flow velocity(CBFV) is an important parameter for study of cerebral hemodynamics. However, a simple and highly similar mathematical model has not yet been established for analyzing CBFV. To alleviate this issue, through TCD examination in 100 geriatric patients with suspected cerebrovascular disease (46 males and 54 females), we established a representative eighth-order Fourier function $V_x(t)$ that simulates the CBFV. The measured TCD waveforms were compared to those derived from $V_x(t)$, an illustrative Kolmogorov-Smirnov test was employed to determine the validity. The results showed that the TCD waves could been reconstructed for patients with different CBFVs by implementing their variable heart rates and the formulated maximum/minimum of $V_x(t)$. Comparisons between derived and measured TCD waveforms suggest that the two waveforms are very similar. The results confirm that CBFV can be well-modeled through an eighth-order Fourier function. This function $V_x(t)$ can be used extensively for a prospective study of cerebral hemodynamics in geriatric patients with suspected cerebrovascular disease.

Cerebrovascular disease has become the second leading cause of death and the leading cause of adult disability worldwide[1,2]. Previous studies have confirmed its close relation with the changes in hemodynamics of the cerebral vessels[3,4]. Functions for the cerebral blood flow velocity(CBFV) are primarily essential for study of cerebral hemodynamics[5,6]. The accuracy of accustomed and suitable functions substantially influences the reliability of the follow-up research results.

However, a simple and highly similar mathematical model for CBFV has not yet been established. Olufsen and colleagues[7] reproduced the full curve of middle cerebral artery blood flow velocity on a beat-by-beat basis as modeled by a windkessel with resistors and a capacitor, but the system must input arterial pressure changes. Ursino *et al.*[8] discussed mathematical models of cerebral blood flow regulation which derives from the interaction and superimposition of several concomitant effects. Previous studies on the cerebrovascular Computational Fluid Dynamics (CFD) chose peripheral vascular blood flow velocity functions as an alternative method for investigating the cerebral blood flow[9,10]. Nevertheless, these functions are too regular to completely apply to CBFV, and could lead to inevitable potential calculation errors. In our previous study, we had successfully established an eighth-order Fourier function which highly fitted cerebral perfusion pressure (CPP) in geriatric patients with suspected cerebrovascular disease[11]. Since both CBFV and CPP are periodic waves based on similar mathematical methods, we set

[1]Department of Neurology, The Third Hospital of Mianyang, Mianyang, Sichuan 621000, China. [2]Department of Neurology, Yongchuan Hospital, Chongqing Medical University, Chongqing 402160, China. [3]Department of Neurology, The First Affiliated Hospital of Chongqing Medical University, Chongqing 400016, China. [4]Institute of Neuroscience, Chongqing Medical University, Chongqing 400016, China. [5]Chongqing Key Laboratory of Neurobiology, Chongqing Medical University, Chongqing 400016, China. *These authors contributed equally to this work. Correspondence and requests for materials should be addressed to H.W. (email: wanghuimysy@126.com) or P.X. (email: xiepeng818@126.com)

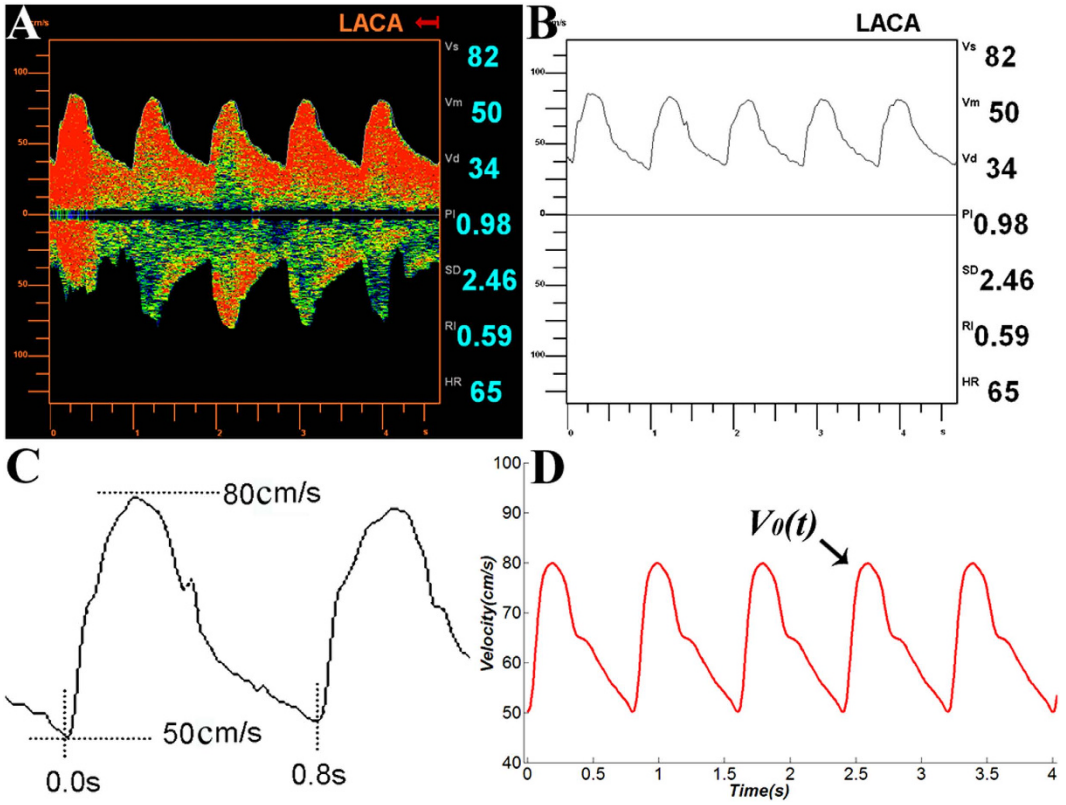

Figure 1. A TCD wave of the left anterior cerebral artery in a patient **(A)** and its black-white picture **(B)**; standardizing a TCD wave, this procedure standardized all cardiac cycles to 0.8 s and all CBFVmax/CBFVmin to 80/50 cm/s **(C)**;the curve of the standardized function $V_0(t)$ **(D).**

up this study to investigate whether the mathematical model could be used to simulate the CBFV in geriatric patients with suspected cerebrovascular disease.

Methods

The study was approved by the Ethics Committee of Chongqing Medical University. Written informed consents were obtained from all participants themselves, the methods were carried out in accordance with the approved guidelines. Our study included patients with suspected cerebrovascular disease who underwent Transcranial Doppler(TCD) examination from January 2014 to December 2014 at our institution. The inclusion criteria were as follows: 1) Patients had signs and symptoms suggestive of cerebrovascular disease. 2) Patients had to undergo TCD examinations. 3) The $CBFV_{max}/CBFV_{min}$ ranged to 30–120/15–90 cm/s, and the heart rate were within a range of 60–100 beats/min. Patients with any stenotic or occlusive disease of the carotid, vertebro-basilar and intracranial arteries along with patients acquiring arrhythmias were excluded from the study. Patients who had a recent onset of moderate to severe stroke, defined as NIHSS score > 4 points were also excluded from the study.

After attaining the TCD results, a sum of nine CBFV waves were bilaterally recorded for each patient: two from the (left and right) anterior cerebral arteries, two from the (left and right) middle cerebral arteries, two from the (left and right) posterior cerebral arteries, two from the (left and right) vertebral arteries and one from the basilar artery.

A TCD wave is an irregular periodic wave (Fig. 1A,B). Considering Parseval's theorem, periodic signals could be summed as the superposition of all the harmonics by applying the triangular form of the Fourier series ($f(t) = a_0 + \sum_{n=1}^{\infty}(a_n \cos nwt + b_n \sin nwt)$, n = 1, 2, 3…)[12]. The eighth-order Fourier function $f(t) = a_0 + \sum_{n=1}^{8}(a_n \cos nwt + b_n \sin nwt)$ was chosen for all TCD waves separately, conferring to the function. All waves were function-fitted using MATLAB 7.0's Curve Fitting toolbox helped fitting with the implementation of the least square method[13,14]. The bandwidth of the curve was set at ±3 cm/s (ordinate) such that all raw data points were located within it.

Since the TCD waves were significantly variable for all the participating patients, it was necessary to standardize all waves to derive at one representative Fourier function with 18 representative coefficients. To accomplish that, 100 patients were randomly selected followed by the standardization of all waves of these patients using the following methods: (1) the abscissa (time) was set up to 0 s at the first nadir; (2) the abscissa (time) to 0.8 s at the second nadir; (3) the ordinate of the nadir to 50 cm/s; and (4) the

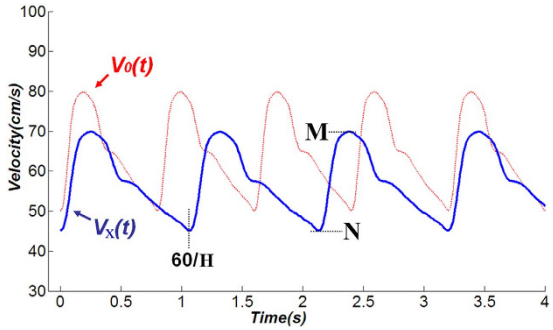

Figure 2. Graphical comparison of $V_0(t)$ and $V_x(t)$: the function $V_x(t)$ can be derived from the lengthening and/or shortening of $V_0(t)$ in the longitudinal and transverse directions, the $V_x(t)$ function can be manipulated to fit the TCD waves for differing CBFVs and heart rates.

Item	Value	
	The derivation group	The validation group
Mean age_SD (range)	68_4(60–80)	68_5(60–80)
Men, n (%)	49(49)	46(46)
Women, n (%)	51(51)	54(54)
Hypertension, n (%)	94(94)	92(92)
Diabetes mellitus, n (%)	12(12)	14(14)
Hypercholesterolemia, n(%)	23(23)	21(21)
Current smokers, n (%)	15(15)	17(17)

Table 1. Demographics of the patients studied.

ordinate of the zenith to 80 cm/s (Fig. 1C). Eventually, this procedure standardized all cardiac cycles to 0.8 s and the $CBFV_{max}/CBFV_{min}$ to 80/50 cm/s.

After this standardization procedure, the 18 standardized coefficients (i.e., w, a0-a8, b1-b8) were obtained by calculating the mean of each coefficient of all new fitted functions. Based on the standardized coefficients, we were able to derive a representative eighth-order Fourier function $V_0(t)$ (Fig. 1D). A function $V_x(t)$ was derived by lengthening and/or shortening of $V_0(t)$ in the longitudinal and transverse directions (Fig. 2). To validate this $V_x(t)$ model, 100 new included patients were chosen randomly with completed TCD examination. The CBFV waves were assessed for each patient by the Fourier function model $V_x(t)$. Comparisons between derived and measured TCD waveforms were tested for the validity.

Statistical Analysis. All statistical analysis was performed by using SPSS 20.0.

Definite integral of the absolute value of the differential function in [0,1] was implemented to compare the coherent function. The single sample Kolmogorov-Smirnov test was employed to test $\int_0^1 |V_{BA}(estimate)(t) - V_{BA}(actual)(t)|dx$, $\int_0^1 |V_{RACA}(estimate)(t) - V_{RACA}(actual)(t)|dx$, $\int_0^1 |V_{LACA}(estimate)(t) - V_{LACA}(actual)(t)|dx$, $\int_0^1 |V_{RMCA}(estimate)(t) - V_{RMCA}(actual)(t)|dx$, $\int_0^1 |V_{LMCA}(estimate)(t) - V_{LMCA}(actual)(t)|dx$, $\int_0^1 |V_{RPCA}(estimate)(t) - V_{RPCA}(actual)(t)|dx$, $\int_0^1 |V_{LPCA}(estimate)(t) - V_{LPCA}(actual)(t)|dx$, $\int_0^1 |V_{RVA}(estimate)(t) - V_{RVA}(actual)(t)|dx$, $\int_0^1 |V_{LVA}(estimate)(t) - V_{LVA}(actual)(t)|dx$ in all patients. The 95% interval <3 was considered as the same curve.

Results

A total of 200 patients were included in our study and the demographic data was listed in Table 1. With a trend of 9 TCD waves per patients, 200 patients received a sum of 1800 TCD waves. Comparative analysis of the 9 waves received from a single patient illustrated that eventhough the 9 TCD waves were characterized with similar rhythms, they were subjected to exhibit miniature differences in the maximum and minimum. On the contrary, the gross arterial study of the 200 patients depicted that: the maximum, minimum, and rhythm of the TCD waves displayed significant differences in all patients; however, as a whole their patterns showed analogy. A typical wave starts at its nadir, then rapidly rises, and on approaching

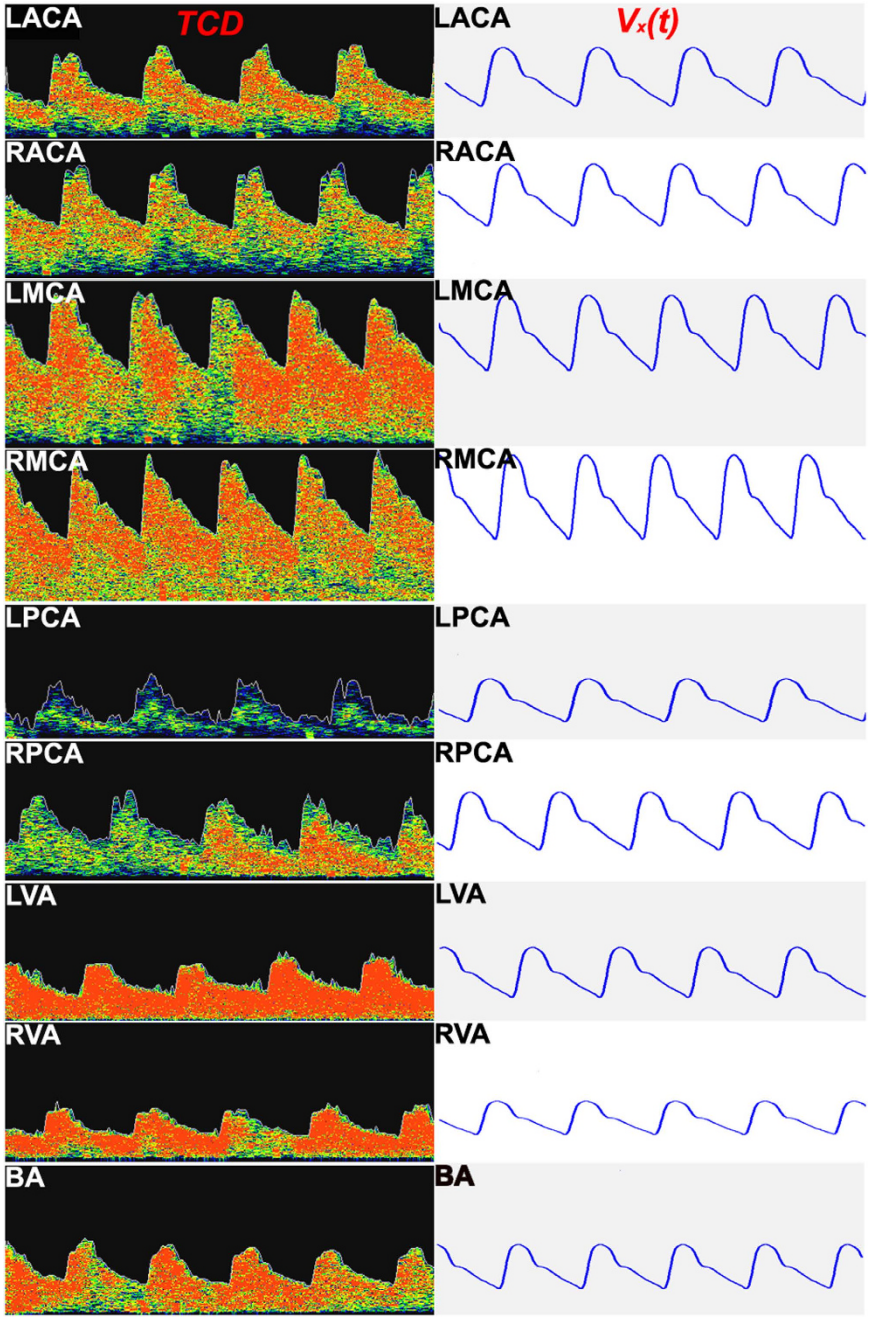

Figure 3. All nine TCD waves of a patient (left); estimated waveforms for each TCD wave based on the function $V_x(t)$ (right); comparisons between estimated and measured TCD waveforms suggest that they are very similar.

its climax follows a slower rate of speed. Some TCD waves exhibited a large angle between fast-ascent and slow-ascent phases. On approaching its culminating point, the TCD waves rapidly declined and then slowed its rate of decline until it reached its nadir (Fig. 3). During the descent phase of the TCD waves, a few waves formed a dicrotic notch, similar to the shape of the Cyrillic letter "*И*".

In order to obtain the common feature of these waveforms, all 900 TCD waves belonging to the derivation group (100 patients, 49 males and 51 females, 60 to 80 years of age, each with 9 waves) were standardized with all cardiac cycles customized to 0.8 s and all $CBFV_{max}/CBFV_{min}$ to 80/50 cm/s. MATLAB 7.0 was able to construct eighth-order Fourier functions so as to fit all the standardized TCD waveforms. After the above procedure, we gained an aggregate of 900 fitting functions (100 patients, each with 9 functions) and on observation, all these new functions demonstrated as follows: these functions not only had the same maximum, minimum and rhythm, but also possessed a consistent waveform morphology; further all corresponded to a single underlying function i.e. $V_0(t)$ pathway.

Coefficient	Mean ± S	Coefficient	Mean ± S
a_0	64.5 ± 3.56	w	7.85 ± 0.04
a_1	−5.154 ± 1.44	b_1	10.962 ± 2.95
a_2	−5.4516 ± 1.45	b_2	1.7574 ± 0.65
a_3	−1.731 ± 0.27	b_3	−0.846 ± 0.64
a_4	−1.5684 ± 0.57	b_4	−0.23976 ± 0.23
a_5	−0.50328 ± 0.43	b_5	−1.0524 ± 0.65
a_6	−0.10014 ± 0.17	b_6	−0.30504 ± 0.11
a_7	−0.035316 ± 0.18	b_7	−0.3963 ± 0.67
a_8	0.16248 ± 0.26	b_8	−0.17118 ± 0.48

Table 2. The mean value of each coefficient of 900 fitted functions after standardization.

Definite integral	P-value	Mean ± S	Confidence interval(95%)	The upper boundary value
$\int_0^1 \lvert V_{RACA(estimate)}(t) - V_{RACA(actual)}(t)\rvert dx$	>0.05	1.63 ± 0.72	[1.53, 1.73]	<3
$\int_0^1 \lvert V_{LACA(estimate)}(t) - V_{LACA(actual)}(t)\rvert dx$	>0.05	1.55 ± 0.48	[1.45, 1.65]	<3
$\int_0^1 \lvert V_{RMCA(estimate)}(t) - V_{RMCA(actual)}(t)\rvert dx$	>0.05	2.05 ± 0.67	[1.94, 2.15]	<3
$\int_0^1 \lvert V_{LMCA(estimate)}(t) - V_{LMCA(actual)}(t)\rvert dx$	>0.05	2.00 ± 0.68	[1.91, 2.10]	<3
$\int_0^1 \lvert V_{RPCA(estimate)}(t) - V_{RPCA(actual)}(t)\rvert dx$	>0.05	1.44 ± 0.43	[1.37, 1.51]	<3
$\int_0^1 \lvert V_{LPCA(estimate)}(t) - V_{LPCA(actual)}(t)\rvert dx$	>0.05	1.65 ± 0.50	[1.58, 1.72]	<3
$\int_0^1 \lvert V_{RVA(estimate)}(t) - V_{RVA(actual)}(t)\rvert dx$	>0.05	1.12 ± 0.33	[1.06, 1.18]	<3
$\int_0^1 \lvert V_{LVA(estimate)}(t) - V_{LVA(actual)}(t)\rvert dx$	>0.05	1.07 ± 0.37	[1.0, 1.14]	<3
$\int_0^1 \lvert V_{BA(estimate)}(t) - V_{BA(actual)}(t)\rvert dx$	>0.05	1.12 ± 0.36	[1.04, 1.20]	<3

Table 3. The single sample Kolmogorov-Smirnov test of nine definite integrals in 100 patients and 95% confidence interval ($\overline{x} \pm s,\ n = 100$)**.**

In order to establish the standardized function $V_0(t)$, the 18 standardized coefficients (i.e., w, a_0–a_8, b_1–b_8) were derived by calculating the mean of each coefficient from the 900 newly fitted functions (Table 2). Based on the standardized coefficients in Table 2, we were able to derive the following representative eighth-order Fourier function: $V_0(t) = 64.5 - [5.154\cos(7.85t) - 10.962\sin(7.85t)] - [5.4516\cos(2*7.85t) - 1.7574\sin(2*7.85t)] - [1.731\cos(3*7.85t) + 0.846\sin(3*7.85t)] - [1.5684\cos(4*7.85t) + 0.23976\sin(4*7.85t)] - [0.50328\cos(5*7.85t) + 1.0524\sin(5*7.85t)] - [0.10014\cos(6*7.85t) + 0.30504\sin(6*7.85t)] - [0.035316\cos(7*7.85t) + 0.3963\sin(7*7.85t)] + [0.16248\cos(8*7.85t) - 0.17118\sin(8*7.85t)]$ (Fig. 1D). $V_0(t)$ has a cycle of $T_0 = 2\pi/7.85 \approx 0.8$s, $\overline{CBFV}_0 = 64.5$cm/s, $CBFV_{0min} = 50$ cm/s, $CBFV_{0max} = 80$ cm/s.

On lengthening and/or shortening of $V_0(t)$ in the longitudinal and transverse directions, the $V_0(t)$ function was manipulated to fit the TCD waves for the varying CBFVs and heart rates (Fig. 2). Thus, in an arbitrary patient X, we could define the $CBFV_{max}/CBFV_{min}$ as M/N (cm/s) and the heart rate as H (beats/min). According to the Fourier function, based on the function $V_0(t)$; CBFV function $V_x(t)$ of this patient X, should be able to conform to the following relationship:

$$V_x(t) = (14.5\mathrm{M} + 15.5\mathrm{N})/30 + (\mathrm{M} - \mathrm{N}) * (V_0(t, H) - 64.5)/30\,(\mathrm{cm/s}).$$

Based upon this formula, we could estimate that the $V_x(t)$ has an average value of (1/30) (14.5 M + 15.5 N) (cm/s), with an ordinate range from M to N, and a cycle of 60/H (s) (Fig. 2).

To validate this $V_x(t)$ model, a validation group (100 patients, 46 males and 54 females, 60–80 years of age) were randomly selected for TCD examinations, and later all TCD waves were function-fitted using MATLAB 7.0. The TCD waveforms were also assessed in each patient by the Fourier function model $V_x(t)$. The estimated TCD waveform and the actual waveform were calculated by using $\int_0^1 \lvert V_{\mathrm{estimate}}(t) - V_{\mathrm{actual}}(t)\rvert dx$. The results suggested that the two waveforms were very similar (Table 3 and Fig. 3). We further validated whether this $V_x(t)$ model can be used for normal subjects. A total of 100 normal subjects (51 males and 49 females, 60–80 years of age) were randomly selected for TCD examinations and all TCD waves were assessed by the Fourier function model. The single sample

Definite integral	P-value	Mean ± S	Confidence interval(95%)	The upper boundary value
$\int_0^1 \left\| V_{RACA\,(estimate)}(t) - V_{RACA\,(actual)}(t) \right\| dx$	>0.05	2.88 ± 0.63	[2.74, 2.99]	<3
$\int_0^1 \left\| V_{LACA\,(estimate)}(t) - V_{LACA\,(actual)}(t) \right\| dx$	>0.05	2.70 ± 0.72	[2.55, 2.83]	<3
$\int_0^1 \left\| V_{RMCA\,(estimate)}(t) - V_{RMCA\,(actual)}(t) \right\| dx$	>0.05	2.69 ± 0.74	[2.54, 2.83]	<3
$\int_0^1 \left\| V_{LMCA\,(estimate)}(t) - V_{LMCA\,(actual)}(t) \right\| dx$	>0.05	2.75 ± 0.67	[2.62, 2.88]	<3
$\int_0^1 \left\| V_{RPCA\,(estimate)}(t) - V_{RPCA\,(actual)}(t) \right\| dx$	>0.05	2.70 ± 0.64	[2.57, 2.81]	<3
$\int_0^1 \left\| V_{LPCA\,(estimate)}(t) - V_{LPCA\,(actual)}(t) \right\| dx$	>0.05	2.73 ± 0.75	[2.58, 2.88]	<3
$\int_0^1 \left\| V_{RVA\,(estimate)}(t) - V_{RVA\,(actual)}(t) \right\| dx$	>0.05	2.59 ± 0.64	[2.45, 2.72]	<3
$\int_0^1 \left\| V_{LVA\,(estimate)}(t) - V_{LVA\,(actual)}(t) \right\| dx$	>0.05	2.52 ± 0.63	[2.39, 2.64]	<3
$\int_0^1 \left\| V_{BA\,(estimate)}(t) - V_{BA\,(actual)}(t) \right\| dx$	>0.05	2.61 ± 0.70	[2.47, 2.75]	<3

Table 4. The single sample Kolmogorov-Smirnov test of nine definite integrals in 100 normal subjects and 95% confidence interval $(\overline{x} \pm s,\ n = 100)$**.**

Kolmogorov-Smirnov test of nine definite integrals in 100 normal subjects were illustrated in Table 4. The results suggested that the estimated TCD waveform and the actual waveform were similar (Table 4).

Discussion

Transcranial Doppler (TCD) is a noninvasive method that is commonly used for detection of the cerebral hemodynamics in patients with suspected neurovascular diseases. It is commonly used in clinical practice due to its relatively very simple operation and good reproducibility. In recent years, TCD has been widely used for measurement of cerebrovascular hemodynamics[15,16]. TCD raw data employ the mean blood flow velocity of the intracranial vessels, which provides important hemodynamic data. MRI might be able to detect cerebrovascular blood flow velocity, but MRI examination is relatively expensive and can not be performed continuous in patients with cerebrovascular diseases. Another advantage of TCD over MRI is that it allows non-invasive dynamic observations of cerebrovascular hemodynamic parameters in a clinical scenario[17,18]. TCD was adopted in this study for an objective and accurate CBFV examination and the function model $V_x(t)$ has successfully derived on the basis of these reliable tests.

Fourier first proposed that any periodic function could be expressed via an arithmetic sum of the constituent sine and cosine functions, which is commonly known as the Fourier series (French: Série de Fourier)[12]. In recent years, Fourier transforms have been applied extensively to numerous set-ups such as medicine, physics, number theories, combinatorial mathematics, signal processing, probability, statistics, cryptography, acoustics and optics[19–21]. CBFV is identical to the other parameters of the cardiovascular dynamics, with its value periodically fluctuating with the heartbeat and such fluctuations is appropriate for its use in the Fourier transforms. The Fourier function in MATLAB 7.0 software package is capable of fitting to integrating all this work. 1–7 order Fourier function curves were smooth and regular, which couldn't be fit to the irregular TCD waves. Therefore, the 1–7 order Fourier function curves were excluded. 9-order Fourier curve fitting produced too much noise from the baseline. Consequently we chose the 8-order Fourier function for each patient's individual TCD wave fitting function. The functions were achieved with efficient fitting results (minimum residual) and minimal noise.

We standardized all variant cardiac cycles to 0.8 s and all $CBFV_{max}/CBFV_{min}$ to 80/50 cm/s in order to obtain the common feature of these TCD waveforms. All standardized TCD waveforms shared a common feature that was very close to $V_0(t)$ pathway and vice versa. Therefore, the $V_x(t)$ function might have been beneficial only to our participants. Further studies are required to demonstrate whether this function could be used for other populations and confirm its reliability. We have selected 100 normal geriatric subjects with a quantitative assessment of sitting errors. The results suggested that the $V_x(t)$ function was quite similar with the actual waveform. The age group of our participants was between 60–80 years old which was the high incidence age of cerebrovascular disease[22]. Thus, $V_x(t)$ could be used widely in the study of cerebrovascular disease.

For the study of cerebrovascular hemodynamics in a particular patient, the CBFV data can directly make use of TCD or MRI. But these data have continuous data points and are not conducive for the subsequent calculations. Therefore, a combined use of the measured data and $V_x(t)$ could be utilized to achieve a double benefit with a reduced effort. In addition, while studying cerebrovascular hemodynamics, we require the function expression instead of raw data points. $V_x(t)$ could also be used in the study of cerebral perfusion pressure(CPP) and/or cerebral vascular resistance(CVR). CPP and CVR changes are slightly complex issues. The CBFV was increased when CPP > CVR and vice versa. The first derivative of $V_x(t)$ was $V'_x(t)$, which could directly manifest changes between CPP and CVR.

Conclusions

Based on the TCD data, CBFV can be well-modeled through an eighth-order Fourier function using MATLAB 7.0. This function $V_x(t)$ can be used extensively for a prospective study of cerebral hemodynamics in geriatric patients with suspected cerebrovascular disease.

References

1. Brea, A., Laclaustra, M., Martorell, E. & Pedragosa, A. Epidemiology of cerebrovascular disease in Spain. *Clin Investig Arterioscler.* **25,** 211–217 (2013).
2. Li, D., Wang, M. L., Li, S. M. & Ling, F. Distribution and risk factors of steno-occlusive lesions in patients with ischemic cerebrovascular disease. *National Medical Journal of China*. **88,** 1158–1162 (2008).
3. Ferini-Strambi, L., Walters, A. S. & Sica, D. The relationship among restless legs syndrome (Willis-Ekbom Disease), hypertension, cardiovascular disease, and cerebrovascular disease. *J Neurol.* **261,** 1051–1068 (2014).
4. Kienreich, K. *et al.* Vitamin D, arterial hypertension & cerebrovascular disease. *Indian J Med Res.* **137,** 669–679 (2013).
5. Berg, P. *et al.* Cerebral blood flow in a healthy Circle of Willis and two intracranial aneurysms: computational fluid dynamics versus four-dimensional phase-contrast magnetic resonance imaging. *J Biomech Eng.* **136,** doi: 10.1115/1.4026108 (2014).
6. Lee, Y. J., Rhim, Y. C., Choi, M. & Chung, T. S. Validation of compliance zone at cerebral arterial bifurcation using phantom and computational fluid dynamics simulation. *J Comput Assist Tomogr.* **38,** 480–484 (2014).
7. Olufsen, M. S., Nadim, A. & Lipsitz, L. A. Dynamics of Cerebral Blood Flow Regulation Explained Using a Lumped Parameter Model. *Am J Physiol Regul Integr Comp Physiol.* **282,** 611–622 (2002).
8. Ursino, M. Mechanisms of Cerebral Blood Flow Regulation. *Crit Rev Biomed Eng.* **18,** 255–288 (1991).
9. Neidlin, M., Steinseifer, U. & Kaufmann, T. A. A multiscale 0-D/3-D approach to patient-specific adaptation of a cerebral autoregulation model for computational fluid dynamics studies of cardiopulmonary bypass. *J Biomech.* **47,** 1777–1783 (2014).
10. Russin, J. *et al.* Computational Fluid Dynamics to Evaluate the Management of a Giant Internal Carotid Artery Aneurysm. *World Neurosurg.* doi: 10.1016/j.wneu.2014.12.038 (2014).
11. Liu, B. *et al.* A Non-Invasive Method to Assess Cerebral Perfusion Pressure in Geriatric Patients with Suspected Cerebrovascular Disease. *PloS one*. **10,** e0120146 (2015).
12. Bracewell, R. N. *The Fourier transform and its applications* (Third Edition) (McGraw-Hill Press, 1999).
13. Alcala-Quintana, R. & Garcia-Perez, M. A. Fitting model-based psychometric functions to simultaneity and temporal-order judgment data: MATLAB and R routines. *Behav Res Methods*. **45,** 972–998 (2013).
14. Yu, H. T. Models with discrete latent variables for analysis of categorical data: a framework and a MATLAB MDLV toolbox. *Behav Res Methods*. **45,** 1036–1047 (2013).
15. Sabayan, B. *et al.* Cerebrovascular hemodynamics in Alzheimer's disease and vascular dementia: a meta-analysis of transcranial Doppler studies. *Ageing Res Rev.* **11,** 271–277 (2012).
16. Roje-Bedekovic, M., Bosnar-Puretic, M., Lovrencic-Huzjan, A. & Demarin, V. Cerebrovascular evoked response to repetitive visual stimulation in severe carotid disease–functional transcranial Doppler study. *Acta Clin Croat.* **49,** 267–274 (2010).
17. Van Amerom, J. F., Kellenberger, C. J., Yoo, S. J. & Macgowan, C. K. Automated measurement and classification of pulmonary blood-flow velocity patterns using phase-contrast MRI and correlation analysis. *Magn Reson Imaging*. **27,** 38–47 (2009).
18. Box, F. M. *et al.* Pravastatin decreases wall shear stress and blood velocity in the internal carotid artery without affecting flow volume: results from the PROSPER MRI study. *Stroke*. **38,** 1374–1376 (2007).
19. Pulkkinen, A. & Tarvainen, T. Truncated Fourier-series approximation of the time-domain radiative transfer equation using finite elements. *J Opt Soc Am A Opt Image Sci Vis*. **3,** 470–478 (2013).
20. Muñoz Morales, A. A., Vázquez, Y. & Montiel, S. Retrieving the optical parameters of biological tissues using diffuse reflectance spectroscopy and Fourier series expansions. *I. theory and application. Biomed Opt Express.* **10,** 2395–2404 (2012).
21. Trajkovic, I., Reller, C. & Wolf, M. Modelling and filtering of physiological oscillations in near-infrared spectroscopy by time-varying Fourier series. *Adv Exp Med Biol.* **737,** 307–313 (2012).
22. Kienreich, K. *et al.* Vitamin D, arterial hypertension & cerebrovascular disease. *Indian J Med Res.* **137,** 669–679 (2013).

Acknowledgements

Thanks is extended to Dr. N.D. Melgiri for his assistance in editing and proofreading themanuscript. Funding: This study was supported by grants from the Natural Science Foundation of the Yongchuan District of Chongqing Municipality (grant no. Ycstc, 2013nc8031), the Foundation of the Chongqing Health and Family Planning Commission (grant no. 20143001), and the National Natural Science Foundation of China (grant No. 81200899).

Author Contributions

B.L. and P.X. conceived and designed the experiments; B.L., Q.L., J.W., H.X., H.G., H.W. and P.X. performed the experiments; B.L., Q.L. and P.X. analyzed the data; B.L., H.W. and P.X. contributed reagents/materials/analysis tools; B.L. and Q.L. wrote the manuscript; B.L. prepared Figs 1–3. All authors reviewed the manuscript.

Additional Information

Competing financial interests: The authors declare no competing financial interests.

How to cite this article: Liu, B. *et al.* A Highly Similar Mathematical Model for Cerebral Blood Flow Velocity in Geriatric Patients with Suspected Cerebrovascular Disease. *Sci. Rep.* **5**, 15771; doi: 10.1038/srep15771 (2015).